Characterization of recombinant human cementum protein 1 (*hr*CEMP1): Primary role in biomineralization

Eduardo Villarreal-Ramírez [a], Abel Moreno [b], Jaime Mas-Oliva [c], Juan Luis Chávez-Pacheco [a], A. Sampath Narayanan [d], Ivet Gil-Chavarría [a], Margarita Zeichner-David [e], Higinio Arzate [a,*]

[a] *Laboratorio de Biología Periodontal y Tejidos Mineralizados, Facultad de Odontología, UNAM, México D.F. 04510, Mexico*
[b] *Instituto de Química, UNAM, México D.F. 04510, Mexico*
[c] *Instituto de Fisiología Celular, UNAM, México D.F. 04510, Mexico*
[d] *Department of Pathology, School of Medicine, University of Washington, Seattle 98195, USA*
[e] *Center for Craniofacial Molecular Biology, University of Southern California, USA*

ARTICLE INFO

ABSTRACT

Cementum protein 1 (CEMP1) has been recently cloned, and *in vitro* experiments have shown functions as regulator of cementoblast behavior and inducer of differentiation of non-osteogenic cells toward a cementoblastic/osteoblastic phenotype. In this study, we have produced a full-length human recombinant CEMP1 protein in a human gingival fibroblast cell line. The purified protein (*hr*CEMP1) has a M_r 50,000. Characterization of *hr*CEMP1 indicates that its secondary structure is mainly composed of β-sheet (55%), where random coil and alpha helix conformations correspond to 35% and 10%, respectively. It was found that *hr*CEMP1 is *N*-glycosylated, phosphorylated and possesses strong affinity for hydroxyapatite. Even more important, our results show that *hr*CEMP1 plays a role during the biomineralization process by promoting octacalcium phosphate (OCP) crystal nucleation. These features make CEMP1 a very good candidate for biotechnological applications in order to achieve cementum and/or bone regeneration.

© 2009 Elsevier Inc. All rights reserved.

Introduction

Cementum is a unique avascular mineralized connective tissue that covers the root surface of teeth and provides the interface through which the root surface is anchored to collagen Sharpey's fibers of the periodontal ligament. Nevertheless, the complex processes that regulate cementogenesis and normal cementum metabolism remain unclear to date. Recent evidence indicates that cementum formation is critical for appropriate maturation of the periodontium [1]. Recently we have isolated and characterized a human cementum protein which we named Cementum Protein 1 (CEMP1), (GenBank Accession No. NP_001041677; HGNC: ID 32553) [2]. Antibodies against this protein recognize the cementoid layer and adjacent cementoblastic cell layer, cementocytes, progenitor cells located near the blood vessels in the periodontal ligament, cells located in the endosteal spaces of human alveolar bone, dental follicle-derived cells and human periodontal ligament cells [2–4]. CEMP1 mRNA is highly expressed in cementoblasts, subpopulations and progenitor cells of the human periodontal ligament [5]. *In vitro* experiments showed that CEMP1 promotes cell attachment, differ-

entiation [6,7], and deposition rate, composition, and morphology of hydroxyapatite crystals formed by human cementoblast cells [7]. Since CEMP1 is synthesized by cementoblast cells and, a restricted periodontal ligament cell subpopulations (cementoblast precursors), it is suggested that this molecule is a cementum-specific biological marker and it might play a role as regulator of cell differentiation. Furthermore, CEMP1 transfection into non-osteogenic cells such as adult human gingival fibroblasts results in differentiation of these cells into a "mineralizing" cell phenotype [8]. Although the physiological function of CEMP1 is not completely understood, it is our hypothesis that this molecule plays an important role during the cementogenesis process and also as an inducer of the formation of mineralizing nodules and calcium deposition during hydroxyapatite formation. Therefore, the aim of the present study was to characterize the physic-chemical characteristics of *hr*CEMP1 expressed in a human gingival fibroblast cell line and determine post-translational modifications and their influence on CEMP1's functional properties during the mineralization process.

Materials and methods

Expression and purification of CEMP1. The open reading frame of CEMP1 (GenBank Accession No. NP_001041677), was subcloned

* Corresponding author. Fax: +52 5556225563.
  E-mail address: harzate@servidor.unam.mx (H. Arzate).

into the pENTR/SD/D vector (Invitrogen, Carlsbad, CA) and the resultant pENTR/SD/D-CEMP1 cDNA construct ligated into a pcDNA40(+) vector pcDNA40-CEMP1(+). Human gingival fibroblasts (HGF) were isolated and grown as previously described [3]. The plasmid pcDNA40-CEMP1(+) was transfected into human gingival fibroblasts cells as described elsewhere [8].

Recombinant human CEMP1 protein collected from conditioned media of HGF expressing CEMP1 was purified by Ni^{2+} affinity chromatography (HiTrap Chelating HP column, Invitrogen, Carlsbad, CA). Determination of protein purity was performed by 12% SDS–PAGE.

Western blot analysis. Recombinant human CEMP1 (10 µg) was separated by 12% SDS–PAGE and electroblotted onto Inmobilon-P (PVDF) nitrocellulose membrane (Millipore Corp., Bedford, MA). Anti-*hr*CEMP1 and anti-6XHis (C-term) polyclonal antibodies were used to specifically identify the CEMP1 gene product and the fused histidines. Peroxidase-conjugated goat anti-rabbit IgG was used and secondary antibody and detection was performed as previously described [2].

Hydroxyapatite affinity chromatography. To determine if *hr*CEMP1 has affinity to hydroxyapatite, an Econo-Pac CHT-II cartridge (1 mL) (Bio Rad, Hercules, CA) was used. The column was equilibrated with 10 mM sodium phosphate, pH 7.2. Fifty micrograms of purified *hr*CEMP1 was loaded and unbound proteins removed with a solution containing 10 mM sodium phosphate, pH 7.2. Bound proteins were eluted with a solution containing 0.05, 0.1, 0.2, 0.3, 0.4 and 0.5 M sodium phosphate, pH 7.2. Fractions were subjected to 12% SDS–PAGE and Western blotting.

Circular dichroism spectroscopy. *hr*CEMP1 protein was dissolved in PBS, pH 7.4, at 200 µg/mL. The concentration was calculated from the absorption at 280 nm using an extinction coefficient of 28,125 M^{-1} cm^{-1} and deduced from the amino acid sequence [9]. CD spectra were recorded in thermostatted (25 °C) quartz cells of 1-mm optical path length within a wavelength range of 190–260 nm using a AVIV62DS spectropolarimeter. The molar ellipticity (θ) expressed in degrees·cm^2 dmol^{-1} was calculated on the basis of a mean residue of M$_r$ 50,000. Five spectra were accumulated to improve the signal to noise ratio. A baseline with buffer (PBS, pH 7.4) was recorded separately and subtracted from each spectrum. The program CONTIN was used to calculate secondary structure content [10].

Dynamic light scattering (DLS). Light scattering experiments were performed using a Zetasizer Nano S (Malvern Instruments, Ltd., UK) molecular sizing instrument which employs a 4 mw, 633 nm semiconductor laser as light source and NIBS technology (Malvern Instruments, Ltd., UK) [11]. During experiments the temperature was held at 25 (0.1 °C) via a Peltier unit. Data analysis was performed using the Zetasizer Nano S DTS software package (Malvern Instruments, Ltd., UK).

Presence of cysteine disulfide bonds. Human recombinant CEMP1 at a 2.5 mM concentration was dissolved with 6 M guanidine–HCl containing 200 mM DTT. The protein was reduced at 37 °C overnight, and boiled for 5 min before the protein was loaded into a gel filtration column (1.5 × 10 cm Sephadex G-10, Pharmacia, Uppsala, SW) equilibrated with 300 mM acetic acid. The reduction state of *hr*CEMP1 was assessed by quantitation of thiols using an assay for dithiodipyridine. Briefly, *hr*CEMP1 was incubated with 6 M guanidine–HCl, 10 mM EDTA, 120 mM Na$_2$HPO$_4$, pH 6.6, and DTPD (4,4'-dithiodipyridine) added to a final concentration of 500 nM. Samples were incubated for 30 min at 25 °C and the A$_{324}$ was monitored to estimate the number of cysteine residues present.

Glycosylation analysis. Carbohydrates contained in *hr*CEMP1 were determined using the ECL glycoprotein detection system (Amersham Biosciences, UK). Briefly, samples were separated by 12% SDS–PAGE and electro-transferred as described above. Oxida-

tion was carried out in the dark with 10 mM sodium metaperiodate dissolved in 100 mM acetate buffer, pH 5.5. Samples were treated with biotin hydrazide to incorporate biotin into the oxidized carbohydrate and biotin was detected by the horseradish peroxidase-conjugated streptavidin system using enhanced chemiluminescence (ECL, Millipore Corp., Bedford, MA).

Release of N-linked oligosaccharides. N-Glycans were released from 200 µg of *hr*CEMP1 by enzymatic cleavage using peptide *N*-glycosidase F (Calbiochem$^®$ Glycoprotein Deglycosylation kit, Merck Biosciences Ltd., Nottingham, UK). The protein was resuspended with 10 µL of 250 mM sodium phosphate buffer, pH 7.0 and 2.5 µL of denaturation solution (2% w/v SDS, 1 M β-mercaptoethanol). The mixture was heated at 100 °C for 5 min. One unit of PNGasa F was added and incubated for 24 h at 37 °C. The *N*-linked glycosylation pattern of *hr*CEMP1 was resolved by 12% SDS–PAGE.

hrCEMP1 phosphorylation. According to 'in silico' analysis, *hr*CEMP1 possesses multiple potential phosphorylation sites. Eighteen phosphorylation sites (10 serine, 8 threonine) were predicted by the NetPhos 2.0 program [2]. Tyrosine is not present in the *hr*CEMP1 amino acid sequence. To determine if serine and threonine phosphorylation is present in *hr*CEMP1, *hr*CEMP1 secreted to the media and purified by Ni^{2+} affinity chromatography was used. Human recombinant CEMP1 was subjected to 12% SDS–PAGE and electrotransfered as described above. Membranes were blocked as described, and incubated with primary polyclonal antibodies against phosphothreonine and phosphoserine (Zymed, San Francisco, CA, USA). After washing, membranes were incubated with the horseradish peroxidase-conjugated goat anti-rabbit IgG secondary antibody. Membranes were washed and detection of secondary antibody performed as previously described.

hrCEMP1 effect on apatite formation. To determine if *hr*CEMP1 promotes apatite formation, a capillary counterdiffusion system was used [13–15]. Briefly, 1% (w/v) agarose gel containing 20 µg/mL of *hr*CEMP1 was poured into the capillaries (0.5 mm diameter and 30 mm long). The ends of the capillaries were injected with 100 mM CaCl$_2$ and 100 mM NaH$_2$PO$_4$. All experiments were carried out at 37 °C. After 7 days, the crystals were recovered by dissolving the gel in hot milli Q water and air-dried.

Energy-dispersive X-ray micro-analysis (EDX). The composition of crystals formed by induction of *hr*CEMP1 into the capillaries was analyzed using a Jeol 5600 scanning electron microscope fitted with a detector of energy dispersive X-ray microanalysis microprobe. All analyses were performed at 20 kV for 300 s [16]. Crystals were analyzed in low vacuum and the calcium/phosphate (Ca/P) ratio was calculated from the intensity of the peaks present in the EDX pattern. After determining the composition of the crystals, they were covered with a thin gold film, 100 nm thick, to avoid electron disturbances that could interfere with the SEM images.

Electron diffraction pattern by transmission electron microscopy. Crystals were mounted on carbon-coated 150-mesh gold grids and examined for diffraction techniques. D-spacings of diffraction patterns were calibrated against those used as gold standard with identical diffraction conditions. The mineral phase was analyzed by means of a JEOL 100 CX analytical transmission microscope employing 100 kV.

Results and discussion

Isolation of human CEMP1 by recombinant expression

Previously, we have expressed *hr*CEMP1 in a prokaryotic expression system; however, this system is not able to express the full-length recombinant CEMP1 [2]. In this study, human recombinant CEMP1 was expressed in human-derived gingival fibroblasts as a secreted 6XHis fusion protein and latter purified

by affinity chromatography using a Ni^{2+} column. The yield of recombinant CEMP1 per liter of serum-free media was about 1 mg. After SDS–PAGE and coomassie blue staining, the protein presented a M_r 50,000 (Fig. 1A, lane 2). The identity of the human recombinant protein was determined by Western blot analysis using a specific polyclonal antibody against the 6XHis tag (Fig. 1A, lane 3) and a specific polyclonal antibody against hrCEMP1 (Fig. 1A, lane 4). Both antibodies recognized a single protein species of M_r 50,000 which is almost twice the theoretical molecular mass deduced from the cDNA sequence (25.9 kDa) [2]. This data shows that we are able to produce the full-length recombinant human CEMP1 in high yields using a human gingival fibroblasts-derived cell line.

hrCEMP1 secondary structure

Circular dichroism of hrCEMP1 showed that the spectra bands present its maximum value at 218 nm. This determines that the secondary structure present in hrCEMP1 is mainly composed of β-sheet. CD spectra analysis revealed 10% α-helix, 32.4% β-anti-parallel, 5.8% β-parallel, 16.7% β-turn and 35% random coil (Fig. 1B). This result was consistent even when different concentrations of trifluoride ethanol (20% and 40%) were used in order to determine if a change in the structure could be induced. Recently, it has been show that proteins with high percentages of random coil structure are multifunctional and allow proteins to have diverse binding properties such as SIBLING and HMGI(Y) [16,17]. This feature might explain why hrCEMP1 regulates crystal growth and composition of hydroxyapatite crystals [7]. CEMP1 also induces the expression of proteins related to mineralization and promotes in vitro osteoblastic and/or cementoblastic cell differentiation of HGF [8].

Dynamic light scattering and cysteine disulfide bonds

Dynamic light scattering analysis revealed that hrCEMP1 aggregates mainly as 6.50 nm particles. Such aggregates are contributed by one type of molecule with a M_r 50,000 (Fig. 1C). Our results showed that hrCEMP1 did not react with sulfhydryl groups. Therefore, all cysteine residues present in hrCEMP1 might be linked to disulfide bridges. Disulfide bridges generally play a role stabilizing protein structure [18–20]. From our results we infer that disulfide bridges contribute to hrCEMP1's secondary structure stabilization.

hrCEMP1 glycosylation and N-linked oligosaccharides

According to in silico analysis (NetNGlyc, neural net bioinformatic program) [12], hrCEMP1 possesses two N-glycosylation sites Asn-X-Ser/Thr in amino acids 20 and 25. After digestion of the protein with PNGase F, our results demonstrate that hrCEMP1 is a glycoprotein with a M_r 50,000 and shifted from M_r 50,000 (Fig. 2C) to a M_r 39,000 species (Fig. 2F and G), which represents 22% of N-glycosylation of hrCEMP1. O-linked glycosylation (Ser/Thr) predicted 13 sites by in silico analysis. After digestion with endo-α-N-acetylgalactosaminidase, α2–3,6,8,9-neuraminidase, β1, 4-galactosidase, and β-N-acetylglucosaminidase, there were no changes in hrCEMP1's M_r (2H). Western blots performed with the digestions described above, cross-reacted with anti-CEMP1 polyclonal antibody (Fig. 2I).

By comparison with the theoretical protein molecular mass for hrCEMP1 (25.9 kDa) deduced from the cDNA sequence, a contribution of 43.5% by post-translational modifications is present in hrCEMP1. However, it is important to consider that V5 epitope and 6XHis tag included into the vector contribute with 5 kDa to the M_r of hrCEMP1. Although the precise role of attached carbohydrates in hrCEMP1 is unknown, glycosylation may affect hrCEMP1's function during the mineralization process. Glycans have been associated to this process because their anionic surface can bind a large number of Ca^{2+} ions and regulate hydroxyapatite crystal growth [21]. Glycans are also implicated in the regulation of endochondral ossification, bone remodeling and fracture healing [22].
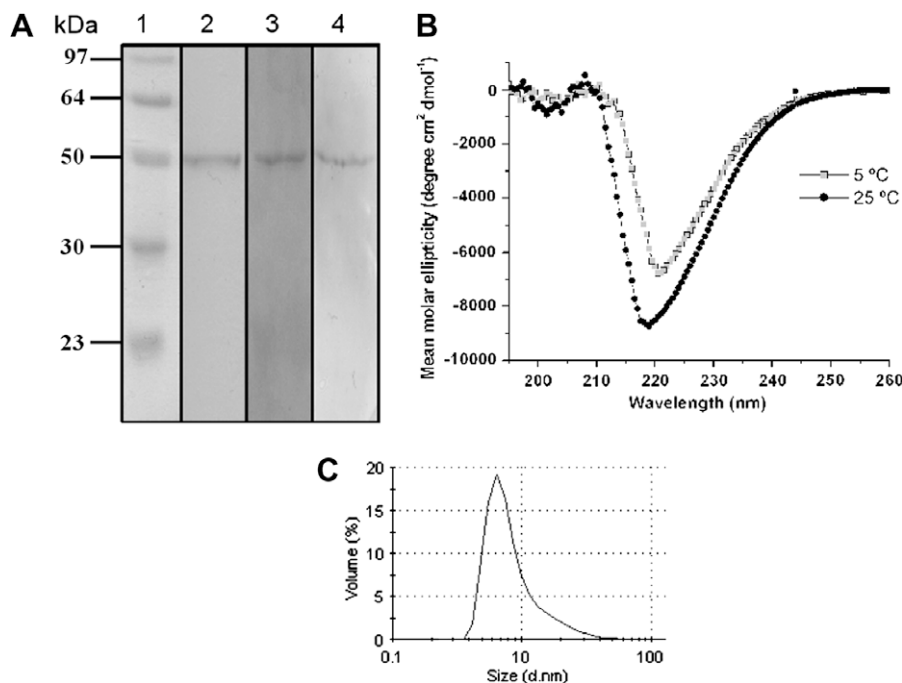
Fig. 1. SDS–PAGE showed a M_r 50,000 species representing hrCEMP1 (A, lane 2). Western blot confirmed the identity of hrCEMP. Anti-6Xhis antibody (A, lane 3), anti-hrCEMP1 (A, lane 4). Circular dichrosim revealed that hrCEMP1 is mainly structured as β-sheet and random coil (B). Dynamic light scattering shows that hrCEMP1 aggregates mainly at 6.50 nm and represents a single molecule of M_r 50,000 (C).
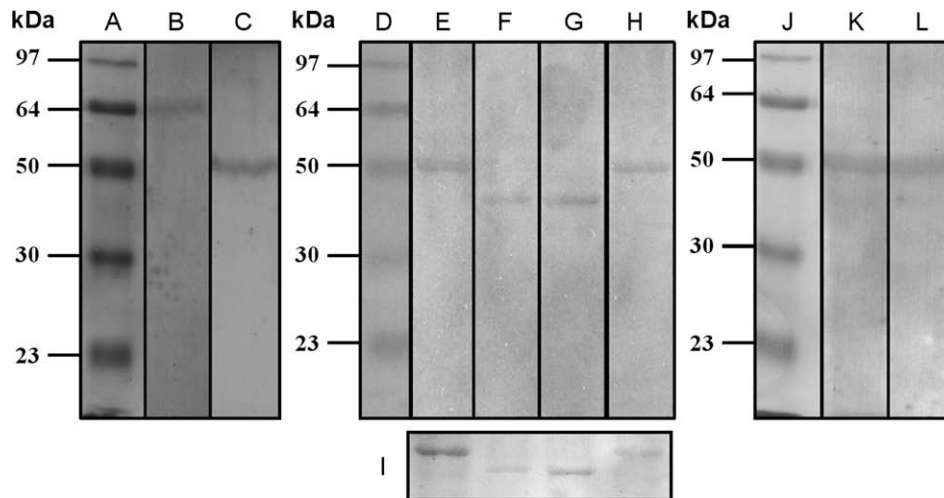
Fig. 2. Transferrin glycoprotein control (B). Human recombinant CEMP1 represents a glycoprotein (C). Deglycosylation of *hr*CEMP1. Human recombinant CEMP1 SDS–PAGE silver stained (D). Incubation of *hr*CEMP1 with a mixture of *N*-linked and *O*-linked deglycosylated enzymes shows a M_r 11,000 difference respect to untreated samples (E). *N*-Deglycosylated enzyme shows a change of hrCEMP1's by 43.5% (F). *O*-Deglycosylated shows no change in *hr*CEMP1' M_r (G). Western blot shows that species mentioned above cross-reacted with anti-*hr*CEMP1 polyclonal antibody (H). Western blot reveals that *hr*CEMP1 is phosphorylated at threonine (I) and serine residues (J).

*hr*CEMP1 phosphorylation

Detection of phosphorylation was done using anti-phospho-serine and threonine antibodies. Our data indicates that both antibodies cross-reacted with the *hr*CEMP1 M_r 50,000 species (Fig. 2K and L). The presence of phosphate favors Ca^{2+} binding to the protein [23,24] and proteins associated to the mineralization process such as: BSP, OPN and DSSP are highly phosphorylated at the threonine and serine residues [25]. This data suggests a role for *hr*CEMP1 at the early stages of mineralization during octacalcium phosphate formation (OCP).

Human recombinant CEMP1 possesses strong affinity for hydroxyapatite

Previous results have shown that CEMP1 plays a role during the mineralization process [7]. The data presented in Fig. 3 shows that *hr*CEMP1 purified from HGF/CEMP1 conditioned media possesses affinity for hydroxyapatite and the species with a M_r 50,000 was recovered only when the column was washed with 300 mM sodium phosphate pH 7.2 (Fig. 3B). The identity of the eluted protein as *hr*CEMP1 was confirmed using the polyclonal antibodies against 6XHis tag and *hr*CEMP1 (Fig. 3C and D), respectively. Proteins not
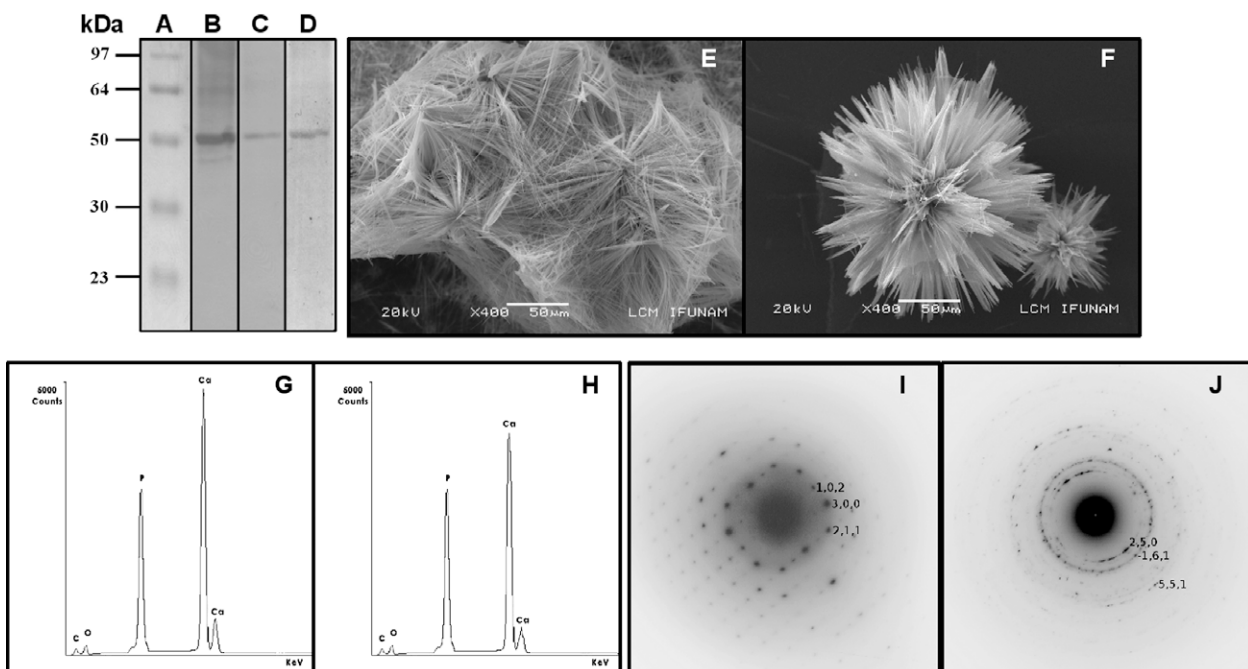
Fig. 3. Hydroxyapatite affinity of *hr*CEMP1. SDS–PAGE Coomassie-stained *hr*CEMP1 (B). CEMP1 binding to hydroxyapatite column (C). Eluted fraction cross-reacted with anti-*hr*CEMP1 polyclonal antibody (D). Hydroxyapatite crystal morphology shows raft-plaque-like features of control crystals (E). Crystals formed in presence of *hr*CEMP acquired a drusa and needle-like morphology (F). EDX analyses reveal prominent peaks of P and Ca^{2+} for control crystals which represent hydroxyapatite (G). Crystals formed in presence of *hr*CEMP1 correspond to OCP (H). Electron diffraction pattern of hydroxyapatite monocrystal (I) and OCP experimental crystals formed under *hr*CEMP1's induction (J).

related to the mineralization process elute at lower concentrations of sodium phosphate [26], whereas proteins implicated with the biomineralization process elute at concentrations between 200 and 300 mM sodium phosphate. Accordingly to this result, hrCEMP expressed in a prokaryote system present the same affinity to hydroxyapatite (data not shown), as the protein expressed in eukaryotic cells. These results indicate that hrCEMP1 possesses intrinsic properties to bind to hydroxyapatite even without post-translational modifications.

hrCEMP1 effect on apatite formation

The morphology of apatite crystals grown in absence of hrCEMP1 had raft-plaque-like shape and microscopic crystals with a globular-spherulite-like shape (Fig. 3E). However, crystals grown in the presence of hrCEMP1 showed drusa-like shape and a combined drusa-like and needle-like morphology (Fig. 3F). Human recombinant CEMP1 induces the formation of polymorphous crystals as confirmed by X-ray diffraction. Elemental analysis performed with EDX determined the Ca/P ratio to be 1.67 for control crystals, equal to the theoretical Ca/P ratio of 1.67 for hydroxyapatite ($Ca_{10}(PO_4)_6(OH)_2$) according to ICDD file: PDF#24-0033 (Fig. 3G). Whereas, experimental conditions using hrCEMP1 determined that the crystals are OCP, ($Ca_8H_2(PO_4)_6 5H_2O$) and EDX elemental analysis determined a Ca/P ratio of 1.33 according to ICDD file: PDF#26-1056 (Fig. 3H). Furthermore, diffraction patterns for the crystals formed under control and experimental conditions were analyzed and index assigned. Diffraction patterns for the control conditions represent hydroxyapatite according to the Miller index (*hkl*: 1 0 2; *hkl*: 3 0 0 and *hkl*: 2 1 1) with interplanar distances of 3.17 Å, 2.72 Å and 2.81 Å, respectively (Fig. 3I). Crystals formed in presence of hrCEMP1 represent OCP according to the Miller index (*hkl*: 2 2 1; *hkl*: −1 2 2 and *hkl*: −4 −4 1) with interplanar distances of 3.74 Å, 2.94 Å and 2.15 Å, respectively (Fig. 3J).

Taken all together, these results demonstrated that biologically active hrCEMP1 plays a role during the biomineralization process, that it is required for the synthesis of needle-shaped OCP crystals and responsible for OCP crystal nucleation activity. OCP is found to be a transient phase during the growth of biological crystals. In small crystals, OCP is completely transformed into HA by hydrolysis and can only be detected in larger crystals because of its slow kinetics of transformation. OCP has also been presumed a necessary precursor of biological apatites in both normal (enamel, dentine, cementum, and bone) and pathological (e.g., phosphatic renal stones) calcifications.

The initial basis of CEMP1's as a possible therapeutic agent rests on evidence showing that CEMP1 has a role during the biological mineralization process of cementum-like tissue, and that induces *in vitro* phenotypic changes from non-osteogenic cells to an osteo-blastic/cementoblastic phenotype [8]. Accordingly, other molecules related to the mineralization process such as BMP-2, 4 and 7 have been established to induce reparative/regenerative mineralized tissue formation [27]. Sustained delivery of BMP-2 using gene therapy has shown to induce bone formation in vivo [28]. Recombinant human amelogenin protein (rHAM(+)), has also been shown to be effective to induce in vivo regeneration of all tooth-supporting tissues after creation of an experimental periodontitis model in dogs, where the recruitment of mesenchymal progenitor cells is a key factor during the formation of regenerated periodontal tissues [29]. Amelogenin and other proteins such as OCN, BSP and OPN have the ability to bind and to regulate hydroxyapatite crystal growth and nucleation as well as to promote mineralization [30,31]. New therapeutic strategies such as the use of PLGA scaffolds for tissue engineering applications could be applied to demonstrate the ability of a single protein to bring about regeneration of mineralized tissues. These strategies could pave the way

for development of new therapeutic devices for treatment of periodontal and bone diseases based on recombinant human CEMP1.

Conclusions

Studies on the function and structure of CEMP1 have been hampered by the difficulties in the isolation of protein from human and/or bovine cementum, due mainly to its low metabolic turnover rate, the amount of tissue being deposited and, its entrapment in hydroxyapatite. In this study, we showed the production, purification and characterization of a full-length hrCEMP1 employing for its synthesis an eukaryotic system. In addition, we demonstrated that CEMP1 is post-translational modified, *N*-glycosylated and phosphorylated. We also showed that hrCEMP1 plays a role during the mineralization process by promoting OCP crystal growth. These results provide the basis for future studies analyzing the potential characteristics of this novel protein towards new therapeutic strategies in order to treat individuals affected by disorders affecting mineralized tissues and to promote regeneration of cementum and/or bone in adult tissues.

Acknowledgments

References

[1] D.D. Bosshardt, S. Zalzal, M.D. McKee, A. Nanci, Developmental appearance and distribution of bone sialoprotein and osteopontin in human and rat cementum, Anat. Rec. 250 (1998) 13–33.
[2] M.A. Alvarez-Perez, S. Narayanan, M. Zeichner-David, B. Carmona-Rodríguez, H. Arzate, Molecular cloning, expression and immunolocalization of a novel human cementum-derived protein (CP-23), Bone 38 (2006) 409–419.
[3] A.S. Narayanan, R.C. Page, Biochemical characterization of collagens synthesized by fibroblasts derived from normal and diseased human gingiva, J. Biol. Chem. 251 (1976) 5464–5471.
[4] M. Zeichner-David, K. Oishi, E. González, Z. Su, V. Zakartchenko, L.S. Chen, H. Arzate, P. Bringas, Role of Hertwig's epithelial root sheath cells in tooth root development, Dev. Dyn. 228 (2003) 651–663.
[5] H. Arzate, L.F. Jiménez-García, M.A. Alvarez-Pérez, A. Landa, I. Bar-Kana, S. Pitaru, Immunolocalization of a human cementoblastoma conditioned medium-derived protein, J. Dent. Res. 81 (2002) 541–546.
[6] H. Arzate, J. Chimal-Monroy, L. Hernández-Lagunas, L. Díaz de León, Human cementum protein extract promotes chondrogenesis and mineralization in mesenchymal cells, J. Periodont. Res. 31 (1996) 144–148.
[7] M.A. Alvarez Pérez, S. Pitaru, O. AlvarezFregoso, J. Reyes Gasga, H. Arzate, Anti-cementoblastoma-derived protein antibody partially inhibits mineralization on a cementoblastic cell line, J. Struct. Biol. 143 (2003) 1–13.
[8] B. Carmona-Rodríguez, M.A. Alvarez-Pérez, A.S. Narayanan, M. Zeichner-David, J. Reyes-Gasga, J. Molina-Guarneros, A. García-Hernández, J. Suárez-Franco, I. Gil Chavarría, E. Villarreal-Ramírez, H. Arzate, Human cementum protein 1 induces expression of bone and cementum proteins by human gingival fibroblasts, Biochem. Biophys. Res. Commun. 358 (2007) 763–769.
[9] P. Mendoza-Espinosa, A. Moreno, R. Castillo, J. Mas-Oliva, Lipid dependant disorder-to-order conformational transitions in apolipoprotein CI derived peptides, Biochem. Biophys. Res. Commun. 365 (2008) 8–15.
[10] S.W. Provencher, J. Glöckner, Estimation of globular protein secondary structure from circular dichroism, Biochemistry 20 (1981) 33–37.
[11] A. Moreno, J. Mas-Oliva, M. Soriano-García, C. Salvador-Oliver, V.M. Bolaños-García, Turbidity as a useful optical parameter to predict protein crystallization by dynamic light scattering, J. Mol. Struct. 519 (2000) 243–256.
[12] N. Blom, T. Sicheritz-Ponten, R. Gupta, S. Gammeltoft, S. Brunak, Prediction of post-translational glycosylation and phosphorylation of proteins from the amino acid sequence, Proteomics 4 (2004) 1633–1649.
[13] L. Silverman, A.L. Boskey, Diffusion systems for evaluation of biomineralization, Calcif. Tissue Int. 75 (2004) 494–501.
[14] C.E. Tye, K.R. Rattray, K.J. Warner, J.A.R. Gordon, J. Sodek, G.K. Hunter, H.A. Goldberg, Nucleation of hydroxyapatite by bone sialoprotein, J. Biol. Chem. 278 (2003) 7949–7955.
[15] J.M. Garcia-Ruiz, Counterdiffusion methods for macromolecular crystallization, Methods Enzymol. 368 (2003) 130–154.

[16] F.J. Cuisinier, R.W. Glaisher, J.C. Voegel, J.L. Hutchison, E.F. Brès, R.M. Frank, Compositional variations in apatites with respect to preferential ionic extraction, Ultramicroscopy 36 (1991) 297–305.

[17] A.K. Dunker, Z. Obradovic, The protein trinity-linking function and disorder, Nat. Biotechnol. 19 (2001) 805–806.

[18] Q.Q. Hoang, F. Sicheri, A.J. Howard, D.S.C. Yang, Bone recognition mechanism of porcine osteocalcin from crystal structure, Nature 425 (2003) 977–980.

[19] E. Hohenester, P. Maurer, C. Hohenadl, R. Timpl, J.N. Jansonius, J. Engel, Structure of a novel extracellular $Ca^{(2+)}$-binding module in BM-40, Nat. Struct. Biol. 3 (1996) 67–73.

[20] B. Kaufmann, S. Müller, F. Hanisch, U. Hartmann, M. Paulsson, P. Maurer, F. Zaucke, Structural variability of BM-40/SPARC/osteonectin glycosylation: implications for collagen affinity, Glycobiology 14 (2004) 609–619.

[21] C.C. Chen, A.L. Boskey, Mechanisms of proteoglycan inhibition of hydroxyapatite growth, Calcif. Tissue Int. 37 (1985) 395–400.

[22] W.J. Grzesik, C.R. Frazier, J.R. Shapiro, P.D. Sponseller, P.G. Robey, N.S. Fedarko, Age-related changes in human bone proteoglycan structure: impact of osteogenesis imperfecta, J. Biol. Chem. 277 (2002) 43638–43647.

[23] M.A. Torres-Quintana, S. Lécolle, M. Goldberg, Effects of inositol hexasulphate, a casein kinase inhibitor, on dentine phosphorylated proteins in organ culture of mouse tooth germs, Arch. Oral. Biol. 43 (1998) 597–610.

[24] S. Jono, C. Peinado, C.M. Giachelli, Phosphorylation of osteopontin is required for inhibition of vascular smooth muscle cell calcification, J. Biol. Chem. 275 (2000) 20197–20203.

[25] M. Zeichner-David, F. Hall, R. Williams, F. Thiemann, S. Yen, M. MacDougall, H.C. Slavkin, Characterization of protein kinases involved in dentinogenesis, Connect. Tissue Res. 33 (1995) 87–95.

[26] S. Hjerten, O. Levin, A. Tiselius, Protein chromatography on calcium phosphate columns, Arch. Biochem. Biophys. 65 (1956) 132–155.

[27] M. Nakashima, Induction of dentin formation of canine amputated pulp by recombinant human bone morphogenetic protein (BMP)-2 and 4, J. Dent. Res. 73 (1994) 15515–15522.

[28] B. Yue, B. Lu, K.R. Dai, X.L. Zhang, C.F. Yu, J.R. Lou, T.T. Tang, BMP2 gene therapy on the repair of bone defects of aged rats, Calcif. Tissue Int. 77 (2005) 395–403.

[29] A. Haze, A.L. Taylor, S. Haegewald, Y. Leiser, et al., Regeneration of bone and periodontal ligament induced by recombinant amelogenin after periodontitis, J. Cell. Mol. Med. (2009), doi:10.1111/j.1582-4934.2009.00700.x.

[30] Q.Q. Hoang, F. Sicheri, A.J. Howard, D.S. Yang, Bone recognition mechanism of porcine osteocalcin from crystal structure, Nature 425 (2003) 977–980.

[31] G.K. Hunter, H.A. Goldberg, Nucleation of hydroxyapatite by bone sialoprotein, Proc. Natl. Acad. Sci. USA 90 (1993) 8562–8565.